# Performance Evaluation of mmWave and Sub-TeraHertz Communication Propagation Path Loss Model Simulation Using NYUSIM

Iwan Donal Paska Manurung<sup>1\*</sup>, Rahmad Hidayat Hadi Subroto<sup>2</sup>, Indrajid Rastra Dewa Brata<sup>3</sup>, and Riri Fitri Sari<sup>4</sup>

<sup>1–4</sup>Department of Electrical Engineering, Faculty of Engineering, Universitas Indonesia Depok, Indonesia 16424

Email: <sup>1</sup>iwan.donal@ui.ac.id, <sup>2</sup>rahmad.hidayat41@ui.ac.id, <sup>3</sup>indrajid.rastra41@ui.ac.id, <sup>4</sup>riri@ui.ac.id

Abstract—Wireless bandwidth becomes increasingly limited, prompting studies to explore frequency bands higher than 100 GHz to enable multi-gigabit communication services and low-latency applications. In this context, Sub-TeraHertz communication offers vast unused spectral resources, enabling unprecedented data rates that can power advanced applications such as ultra-highdefinition video streaming, holographic communication, and massive machine-type communications. Therefore, the research aims to review the performance of millimeter wave (mmWave) and Sub-TeraHertz signal propagation in a dense environment such as an industrial complex, addressing major challenges including high propagation losses, atmospheric absorption, and signal blockage. By using NS-3 to simulate different scenarios, both inside and outside the factory, the analysis aims to characterize the channel performance and provide insight into the potential of Sub-TeraHertz communication for industrial environments. Through comprehensive simulation using the Urban Micro (UMi) scenario, the analysis models the propagation loss from a dense environment with maximum blockages. In addition to the received signal as a function of transmitter-receiver distance, the results show that the number of blockages between the transmitter and receiver, the mobility of the receiver, the frequency band, and the spectrum bandwidth substantially affect the propagation loss of signal transmission in mmWave and Sub-Terahertz Bands. These findings highlight the importance of considering indoor-outdoor disparities, blockage effects, and environment-specific network design when deploying high-frequency communication systems. The research also provides a foundation for future research to explore mitigation techniques to enhance reliability and coverage in complex industrial deployments.

Index Terms—mmWave, Sub-TeraHertz, Propagation Loss Model, New York University Channel Model Simulator (NYUSIM), Industrial Complex

Received: Feb. 02, 2025; received in revised form: May 09, 2025; accepted: May 09, 2025; available online: Sep. 23, 2025. \*Corresponding Author

#### I. Introduction

Vast increment of high-speed communication and the high growth of user demands are causing challenges and opportunities. The need for massive bandwidth capacity with limited frequency channels challenges studies and experts to exploit millimeter wave (mmWave) and Sub-TeraHertz frequency bands as future alternatives [1, 2]. The mmWave band offers ultra-wide spectrum channels and provides significant increases in communication capacity compared to sub-6 GHz microwave bands. However, mmWave propagation is highly susceptible to Line-of-Sight (LOS) blockage and diffraction, having a relatively high probability of outage [1]. Following the discussion, microwave communications are relatively immune to these factors.

Additionally, wireless bandwidth limitation is becoming a critical problem for 5G networks. The current demand for 6G networks is to provide multi-gigabit communication services that support high-speed communication and low-latency applications, such as High-Definition Television (HDTV), Ultra-High Definition Video (UHDV), and Industrial Internet of Things (IoT), among others. Most current studies focus on the 28, 38, and 60 GHz bands, as well as the E-band (71-76 and 81-86 GHz) [1]. Moreover, the increasing demand for higher data rates, low latency, and improved network capacity in current communication systems has pushed experts toward the use of higher frequency bands, particularly in the Sub-TeraHertz range [3]. Sub-TeraHertz communication, operating in the frequency range of approximately 100 to 300 GHz, has surfaced as a promising candidate to address bandwidth scarcity in conventional wireless communication systems.

The mmWave communications at 28 and 73 GHz

frequencies with up to 2 GHz of bandwidth can support data exchange up to multi-gigabit data rates per second. Institute of Electrical and Electronics Engineers (IEEE) plans to utilize frequencies more than 100 GHz for 6G and further to enable the increasing demand for ultra-high user data rates exceeding tens of gigabits per second [4]. Sub-TeraHertz communication offers vast unused spectral resources, enabling unprecedented data rates to support applications, such as ultra-highdefinition video streaming, holographic communication, and massive machine-type communications. Furthermore, the shorter wavelengths associated with Sub-TeraHertz frequencies allow the development of highly directional antennas, facilitating beamforming methods to improve spatial reuse and mitigate interference [5]. Sub-TeraHertz frequency has a vast untapped spectrum as a promising future development in wireless communications, which can meet the high bandwidth demand and support ultra-wideband communications [6]. However, Sub-TeraHertz technology requires solutions to overcome certain challenges, such as special operating conditions for propagation, specialized commercial Radio Frequency (RF) components, and high-power steerable antennas [7].

The characteristics of mmWave and Sub-TeraHertz communication are reviewed as follows. First, regarding large bandwidth, standardization of several frequency bands has been conducted, and currently, there are only several spectrums in use, which are assumed to have a low chance of interference. For instance, the 28 and 39 GHz bands can be assigned with 50 MHz up to 400 MHz of bandwidth. Additionally, higher frequencies are expected to support a wider bandwidth [8]. Second, it enables large number of antenna arrays. The short wavelength enables the use of compact antenna arrays, allowing the incorporation of mmWave technology into a physically small form factor. These small-sized antenna elements enable electrically large array construction to achieve higher performance and finally contribute to the development of Multi-User, Multiple-Input, Multiple-Output (MU-MIMO) [9]. Third, there is a blockage sensitive. Blockage can cause significant effects in Sub-TeraHertz signals compared to other frequency bands, such as walls, doors, and even the human body [10]. These characteristics make outdoor antenna has a low chance of covering indoor users. Blockages in Sub-TeraHertz can cause differences between LOS paths and Non-Lineof-Sight (NLOS) paths. Lastly, they have higher power consumption. Some device components in mmWave consume more power due to transmitter and receiver hardware designs. However, the increase in circuit power consumption can be compensated for by a vast

increase in data rate [11].

Although the development of mmWave and Sub-TeraHertz faces many challenges, industry and academia are working to map out possible solutions. High propagation losses, atmospheric absorption, and susceptibility to blockage require innovative solutions in terms of device design, propagation modeling, and network architectures. Relating to the discussion, Path Loss at Sub-TeraHertz frequencies is generally greater than at lower frequencies. It is because higher frequencies tend to be more vulnerable to physical barriers such as buildings and vegetation. For instance, a previous study shows that at a frequency of 140 GHz, the typical Path Loss rises by 10.7 dB in LOS situations and 6.0 dB in NLOS scenarios [12]. Sub-TeraHertz frequencies also pass through greater scattering and dispersion. Scattering from uneven surfaces and various obstacles can lead to a broader signal dispersion, impacting the quality of the signal received [13]. Additionally, advancements in materials, semiconductor technologies, and modulation schemes are necessary to achieve efficient transmission and reception at these frequencies.

Current literature on the use of frequencies >100 GHz is still very limited, as most of the studies are focused on the exploitation of <100 GHz channel systems. The research is investigating specifically Sub-TeraHertz channel frequencies at >100 GHz in an industrial complex. The selection of frequency channels is closely related to the selection of deployment contexts in industrial areas. Industrial complexes are generally densely populated areas that require massive high connectivity. In addition to human-to-human communication, industrial areas also require a lot of human-to-machine and machine-to-machine communication. The use of sensors, high-quality cameras, machinery control, and factory management requires high-speed data as well as low-latency communication that needs to be run continuously in high quantities and qualities. The development of Sub-TeraHertz in the industrial complex is an interesting topic and can contribute to the transition from mmWave to Sub-TeraHertz communication.

The implementation of Sub-TeraHertz networks requires rigorous study, planning, and understanding of the relatively new technological concepts, as Sub-TeraHertz behaves differently from sub-6 GHz networks. Many of the studies in these areas focus on developing core technologies and relevant enablers. Moreover, network designers still face dramatic challenges in developing implementation design. Many analyses focus on developing a statistical model of signal performance based on field measurements [14], which is presented later in the study methods. This

analysis found a lack of studies related to how to design Sub-TeraHertz communication using known statistical models.

Motivated by the potential for different implementation requirements, the research presents a comprehensive simulation of multiple scenarios for Sub-TeraHertz networks in the general field implementation. The work in this analysis can help network designers to perform preliminary studies on designing communication systems in high-density clutter areas. However, the research does not provide any statistical analysis of mmWave or Sub-TeraHertz characterization in an industrial complex. The analysis focuses on characterizing signal performance using a previously studied propagation model by the New York University Channel Model Simulator (NYUSIM) team.

#### II. RESEARCH METHOD

A. New York University Channel Model Simulator (NYUSIM) Implementation in NS-3

NS-3, which is a new development of NS-2, is a discrete-event network simulator [15], a well-known tool for communication as well as networking studies and practitioners. NS-3 is mainly used for analyzing and developing a wide range of applications in the network domain, from simulating complex networks, assessing security systems, to developing and testing novel protocols. Additionally, NS-2 and NS-3 are open-source tools used by the networking community to solve many network-related problems. NS-3 is publicly available to be downloaded from nsnam.org, and is backed up by active community studies worldwide from both industry and academia. The community has developed and enriched NS-3 core functions with many supporting modules and features. Currently, NS-3 can be used to simulate a wide variety of networks, both wireless and wired, protocols, and algorithms. Comprehensive documentation and tutorials are also available on the NS-3 website [16].

NS-3 is developed in C++, where all core and supporting modules are coded in C++ and structured in multiple C++ classes. The modules are organized in separate folders inside src in the installation directory. The different modules can be combined as needed (modular) to simulate a network scenario. This modular characteristic makes NS-3 a very useful tool, specifically for cross-layer design and analysis. Each module contains both documentation and source code, as the code is organized into multiple folders that contain models, helpers, examples, and tests. This file hierarchy can help studies of NS-3 to understand the working principles of each module, examine the

provided examples, and start making code changes as required [16].

NS-3 has been supported and developed with a wide variety of modules. The component is now equipped with numerous collections of modules, including antenna, Ad hoc On-Demand Distance Vector (AODV), network, Internet, point-to-point, applications, Wi-Fi, WiMAX, statistics, and many more specialized modules. However, there is no definitive or publicly stated number of available NS-3 modules. In addition to the built-in libraries, NS-3 has also been used as a basis for various external study projects. These projects are managed as well as developed by separate parties and are different groups from NS-3 maintainers, but they use NS-3 as the basis for library development. Some of the quite well-known external projects, such as LTE-EPC Network Simulator (LENA) project [17], Named Data Networking (NDN) Simulator (ndnSIM) [18], NYUSIM - mmWave and Sub-TeraHertz channel simulators [19], Quantum Key Distribution Network Simulation (QKDNetSim) module [20], and many more [21]. However, the research specifically uses the mmWave module and the extended library NYUSIM.

NYUSIM was developed by New York University (NYU) WIRELESS in 2016 as an extension module for the NS-3 simulator for the open-source mmWave and Sub-TeraHertz channel simulators. NYU Wireless, a wireless communications study center at the New York University Tandon School of Engineering, has claimed that NYUSIM is the first wireless channel simulator capable of generating real-world wireless channels higher than 100 GHz. NYUSIM is an opensource mmWave wireless channel simulator that is publicly available to download and use by global industrial and academic institutions. NYUSIM is developed in MATLAB and NS-3, as the MATLAB version of NYUSIM can simulate drop-based as well as spatial consistency-based channel simulations with human blockage [22]. However, only the drop-based channel simulation without human blockage was for the NS-3 version.

The propagation model, in general, is determined by three components as follows. First, the Channel Condition model is used to determine LOS/NLOS conditions. Second, Path Loss and Shadowing models are used to model power loss due to propagation distance as well as blockage. Finally, Multipath and Fading models are used to model power loss due to the influence of various types of named models.

B. New York University Channel Model Simulator (NYUSIM) Module Overview

In NS-3, the wireless channel is managed by the Propagation and Spectrum modules. The propagation module defines the PropagationLossModel interface to compute large-scale fading. To handle smallscale fading, Spectrum defines the SpectrumPropagationLossModel interface. The extended libraries NYUChannelConditionModel as well as NYUPropagationLossModel should be added to the Propagation module. Meanwhile, NYUChannelModel and NYUSpectrumPropagationLossModel should be added to the Spectrum module to enable NYUSIM in NS-3. Concerning the Antenna module, NYUSIM uses the ThreeGppAntennaArrayModel, a generic antenna design similar to the 3rd Generation Partnership Project (3GPP) Spatial Channel Model (SCM) model [23]. The implementation of NYUSIM in NS-3 is reviewed in three parts:

- The Probability of LOS/NLOS channel condition is determined by the NYUChannelCondition-Model.
- 2) Path Loss and Shadowing effects are determined by NYUPropagationLossModel,
- The small-scale fading (fast fading and frequency selective fading) is modeled by the NYUSpectrumPropagationLossModel.

The NYUSIM module in NS-3 can be integrated with other modules according to the needs of a given simulation. In the research, the built-in Building module is employed to represent buildings as blockage components. This module is designed to model both indoor and outdoor environments, allowing for more realistic wireless network simulations. It enables researchers to define key building parameters such as width, height, depth, number of floors, wall type, and number of rooms, and to place network nodes either inside or outside the structures. The module also accounts for the impact of walls, floors, and construction materials on signal attenuation, while distinguishing between line-of-sight and non-line-of-sight conditions. Such functionality is particularly valuable for identifying common reception issues, as indoor user devices often encounter very different propagation behavior compared to that outdoors. By incorporating these spatial and structural features, the Building module provides a strong framework for analyzing wireless network performance in complex indoor and urban environments.

#### C. Line-of-Sight (LOS) Probability Models

The LOS Probability or Channel Condition models are used to determine LOS and NLOS conditions. In

the 3GPP Channel model, LOS Probability models are a function of the transmitter-receiver (TX-RX) separation distance and sometimes a function of the TX as well as RX heights. The model is formulated from the sub-6 GHz LOS probability model developed by 3GPP [24]. Moreover, the 3GPP Channel model utilizes a Stochastic Channel Model (SCM) for the channel generation procedure and is a widely adopted standard for the mmWave band, extending up to 100 GHz. The 3GPP SCM provides a set of statistical parameters and Multipath Channel Impulse Response (CIR) to generate link-level modeling for Urban Micro (UMi), Urban Macro (UMa), Indoor Hotspot (InH), and Indoor Factory (InF) environment scenarios. Most of the current available simulation tools used by studies and engineers heavily rely on the 3GPP SCM procedures.

The LOS Probability models in NYUSIM are highly dependent on 2D TX-RX separation and frequency-independent [25]. The NYUSIM LOS probability model for outdoor is modeled based on radio propagation field measurements observed at 28 and 73 GHz in New York City. Following the discussion, Tx-Rx locations are selected from the measurement data, and ray tracing is used to determine how the path between TX and RX is in LOS/NLOS [26]. NYUSIM supports 0.5-150 GHz, a wider frequency range than 3GPP SCM, and is used for all 3GPP-listed scenarios, such as UMi, UMa, Rural Macro (RMa), InH, as well as InF scenarios. The NYUSIM channel model also provides a more realistic and accurate probability model than the 3GPP SCM [2, 27].

The NYUSIM Channel Condition model in NS-3 is implemented under the ChannelCondition class. This ChannelCondition is then further developed into five different scenarios after the 3GPP-listed scenarios. They are as follows:

- 1) NYURmaChannelConditionModel is used for the RMa LOS scenario,
- 2) NYUUmaChannelConditionModel is used for the UMa LOS scenario,
- 3) NYUUmiChannelConditionModel is used for the UMi LOS scenario,
- NYUInHChannelConditionModel is used for the InH LOS scenario, and
- NYUInFChannelConditionModel is used for the InF LOS scenario.

## D. Path Loss and Shadowing Models

Path Loss defines the reduction in power density of a signal wave as it propagates through the channel. Models are developed to explain or facilitate understanding of how signal attenuation is influenced

by various factors, including distance, frequency, and environmental conditions [28]. Moreover, the received power is a function of distance between antennas (d) and wavelength ( $\lambda$ ), known as Friis' Law [29], which is expressed in Eq. (1). The  $P_T$  and  $P_R$  signify transmitted as well as received power. Then,  $G_T$  and  $G_R$  represent the antenna gains at the TX and RX ends. The  $\pi$  is the mathematical constant pi, and  $d_{3D}$ signifies the spatial distance between TX and RX. NYUSIM models all scenarios except RMa using the close-in (CI) free space reference distance model. In addition to Free Space Path Loss (FSPL), there is additional attenuation due to atmospheric attenuation (AT), outdoor-to-indoor loss (O2I), foliage loss (FL), and shadow fading  $(\chi)$  [27]. FSPL(f, 1m) represents the free space Path Loss at a TX-RX separation of 1 meter at frequency f. Relating to the process, the Path Loss model  $(PL^{CI})$  as a function of frequency (f)and distance (d in meter) in NYUSIM is expressed in Eq. (2).

$$P_{R}(d,\lambda) = P_{T}G_{T}G_{R}(\frac{\lambda}{4\pi d_{3D}})^{2}, \qquad (1)$$

$$PL^{CI}(f,d)[dB] = FSPL(f,1m)[dB] + 10\eta \log_{10}(d) + AT[dB] + O2I[dB] + FL[dB] + \chi_{\sigma}^{CI}[dB]. \qquad (2)$$

The propagating signal in shadowing models is adjusted by objects that block, diffract, or reflect the transmission path, such as buildings or terrain. These forms of models help to get a better idea of how the propagation condition affects the transmitted signal. For instance, shadowing caused by buildings in urban areas has a significant impact on total service coverage. Empirical models are designed to estimate excess loss due to this form of shadowing [30].

## E. Multipath and Small-Scale Fading Models

Multipath fading is a term to define a condition in which transmitted signals reach the receiving antenna with different paths due to reflection, diffraction, and scattering around the obstacles. This phenomenon leads to various signal paths and causes fluctuation of signal strength and quality when these paths interfere with each other constructively or destructively. Numerous studies have been conducted to minimize the Multipath phenomenon and reduce its impact on signal attenuation and reflection [31].

Small-scale fading represents a condition when a signal is transmitted from a transmitter to a receiver. The process experiences multiple signal paths due to reflection, diffraction, and scattering from objects in the environment. The phenomenon causes rapid fluctuations in the amplitude and phase of the signal

over short distances or periods, typically on the order of the wavelength of the signal. This type of fading is influenced by the movement of the transmitter, receiver, or surrounding objects and is often modeled using statistical distributions [32]. Small-scale fading is further categorized into flat-fading and frequency-selective fading, depending on whether the signal bandwidth is smaller or larger than the coherence bandwidth of the channel [33].

In the NYUSIM channel model, Time Clusters (TC) are composed of Multipath Components (MPCs) traveling closely in time (tens or hundreds of nanoseconds) [14], which propagate to a common direction in a space called the Spatial Lobe (SL) [29]. Using measurement data, NYU WIRELESS develops a statistical model to generate the temporal and spatial characteristics of the channel, known as the Time Cluster Spatial Lobe (TCSL). Moreover, TCSL is used to generate TC and SL statistical data.

#### F. Related Works

The deployment of mmWave wireless communication systems in industrial complexes has faced several challenges. Interference, small coverage, blockage, delay, and retransmission are among the major issues. The number of coexisting technologies and the density of existing transceivers add more interference issues to both existing and new deployments of wireless systems [34]. Typical buildings in factories often have more clutter, which severely degrades signal performance due to the high probability of NLOS and partial LOS communication links. In this context, human density inside buildings also introduces additional shadowing effects, as mmWave is highly susceptible to shadowing components, even small blockages such as the human body, which can significantly impact mmWave signal performance. Based on field measurement at a 73 GHz point-to-point link, the human body increases signal attenuation from around 11.5dB to 15.8dB [35].

The wavelength reduces as the frequency increases, where atmospheric absorption, as well as rain, degrades mmWave and Sub-TeraHertz signals much more than microwave frequencies, including 6 GHz and lower. However, high directional antennas in both TX as well as RX and shorter distances of TX-RX separation compensate for the loss and attenuation caused by atmospheric loss [27]. Higher frequencies experience increased molecular absorption losses in the context of this discussion. At very short distances (tens of meters), mmWave and Sub-TeraHertz are only affected by FSPL as the dominant loss. On the other hand, molecular absorption losses increase progressively at

longer distances. Molecular absorption is strongly dependent on the water vapor level in the atmosphere since water vapor absorbs energy efficiently [5].

In the specific case of industrial complexes, wireless communication is generally influenced by the high density of clutter such as room, wall, human, machine, desk, and others. The research examines some previous work related to the process of the analysis. The first study has used field measurements across factories in New York City using 142 GHz. Furthermore, the analysis also explores spatial or temporal channel responses at 5-85 meters of TX-RX separation for both LOS as well as NLOS scenarios with 1 GHz bandwidth and steerable directional antennas. All measurements are conducted in 82 TX-RX locations, including 30 LOS and 48 NLOS locations. In addition, the process analyzes Path Loss, Path Loss Exponent (PLE), Cross-Polarization Discrimination (XPD) characterization, and potential power gain due to Passive Reflecting Surfaces (PRS) [6].

The second analysis has studied Industrial IoT in industrial environments with a high density of clutter and objects. It uses a hybrid deterministic 3D Ray Launching to provide precise wireless channel characterization. Following the process, the proposed method is compared to a real measurement scenario. The communication link is configured for 433 MHz, 868 MHz, 2.4 GHz, and 3.5 GHz, with both LOS and NLOS scenarios. The research analyzes coverage and capacity, interference mapping, and delay spread distributions [34].

The third study has presented an overview of 28 GHz bands in the smart warehouse environments using field measurement in three different scenarios, including an intelligent forklift truck scenario, a stacking and shuttle car scenario, as well as an Automated Guided Vehicles (AGVs) scenario. It analyzes Path Loss, Root Mean Square (RMS) delay spread, and Rician K factor. It shows that the density and mobility of vehicles in smart warehouses increase the probability of the Obstructed Line-of-Sight (OLOS) state compared to industrial scenarios. As a result, proper and accurate path planning is critical to minimizing OLOS conditions [4].

#### G. Simulation Setup

The 3GPP Technical Report (TR) 38.901 defines a stochastic channel model for the 0–100 GHz frequency band, which is used for mobile connectivity and access networks. This standardized model is used to generate large-scale and small-scale fading models. TR 38.901 also defines multiple scenarios for channel model calibration and testing. The detailed scenarios defined by TR 38.901 are described as follows:

TABLE I PATH LOSS MODEL.

| Parameters            | Values                 |
|-----------------------|------------------------|
| Path Loss scenario    | NYUSIM UMi             |
| Frequency Bands (GHz) | 73, 100, 120, 140      |
| Bandwidth (MHz)       | 200, 400, 600, and 800 |
| Blockage              | Enable                 |

- UMi street canyon defines an outdoor/indoor scenario with Inter-Side-Distance (ISD) of 200 m and Base Station (BS) antenna height around 10 m,
- 2) UMa defines outdoor/indoor scenarios with an ISD of 500 m and BS antenna height of around 25 m.
- RMa defines rural scenarios as a larger coverage.
   Ideally, it is used for frequency up to 7 GHz with BS height around 35 m,
- 4) Indoor-Office defines an indoor scenario with an ISD of 20 m and a BS antenna height of around 3 m (ceiling),
- 5) InF defines indoor scenarios, focusing on factory clutter and BS antenna heights of around 5–25 m (factory ceiling).

Concerning the purpose of the simulation, the researchers focus on the UMi Street Canyon scenario. It is best for outdoors in a larger area coverage with a BS antenna positioned far above the rooftop of the building and lower frequency bands to reach larger coverage. In the analysis, the InF scenario is considered an alternative. However, the UMi scenario is proven to be most relevant for evaluating channel model performance for user terminals around a factor building.

#### H. Simulation Parameters

A total of three parameter models is used to simulate all the scenarios. The parameter for the Path Loss model is shown in Table I. Table I describes the simulation scenarios used, with four frequency scenarios: 73 GHz, 100 GHz, 120 GHz, and 140 GHz. For each frequency scenario, the bandwidth is set to four subscenarios: 200 MHz, 400 MHz, 600 MHz, and 800 MHz. In each scenario and sub-scenario, 3GPP TR 38.901 UMi is implemented with the blockage setting enabled.

Then, the ENodeB (TX) and UE (RX) models are in Table II. It describes the air interface settings between the base station represented by EnodeB (the terminology representing a base station by 3GPP in Long Term Evolution (LTE) cellular networks) and User Equipment (UE). On the TX side, an Isotropic/Omnidirectional antenna with a transmit power of 30 dBm is used, installed at a height of 15 m with 3-D coordinates at (150, 200, 15). The TX mobility

TABLE II
ENODEB BASE STATION (TX) AND USER EQUIPMENT (UE)
(RX) MODELS.

| Parameters            | Values                               |
|-----------------------|--------------------------------------|
| TX Antenna type       | Isotropic/Omnidirectional            |
| RX Antenna type       | Isotropic/Omnidirectional            |
| TX Gain (dBm)         | 30                                   |
| RX noise figure (dBm) | 9                                    |
| TX Position           | (150, 200, 15)                       |
| TX Antenna height (m) | 15                                   |
| RX Antenna height (m) | 1 and 11                             |
| TX-RX Separation (m)  | 50-50                                |
| LOS type              | LOS and NLOS                         |
| TX Mobility           | Constant Position                    |
| RX Mobility           | Constant Velocity (300m/s in Y-axis) |

TABLE III BUILDING BLOCKAGE MODEL.

| Parameters                | Values          |
|---------------------------|-----------------|
| Number of buildings       | 13              |
| Building type             | Commercial      |
| Windows type              | Without windows |
| Building height (m)       | 20              |
| Number of Floors          | 2               |
| Number of Rooms in X-axis | 2-12            |
| Number of Rooms in Y-axis | 2-12            |

is also set at a constant position. On the RX side, an Isotropic/Omnidirectional antenna with a noise figure of 9 dBm is used, positioned at a height of 1 m (first floor) and 11 m (second floor). The RX mobility is set to move at a constant velocity of 300 m/s along the Y axis across the outdoor and indoor areas. The RX mobility also represents LOS and NLOS conditions, thus simulating outdoor to indoor loss.

Lastly, the Building Blockage model is presented in Table III. It describes the blockage conditions represented by 13 adjacent two-story buildings, like in a real industrial complex. Each building is configured as a windowless commercial building, is 20 m tall, and has 2–12 rooms per floor.

## I. New York University Channel Model Simulator (NYUSIM) Parameters

Following the parameters mentioned earlier, NYUSIM is configured as follows. First, in the Path Loss model, class NYUPropagationLossModel is set to NYUUmiPropagationLossModel to the **NYUSIM** UMi scenario. Class NYUPropagationLossModel::ShadowingEnabled set to true to enable blockage in Path calculations. After the process, Class NYUChannelModel::SetFrequency used is to define the center frequency. The center frequency is configured accordingly, following the simulation scenario during the process. The Class

NYUChannelModel::SetRfBandwidth is used to define the bandwidth and is configured accordingly after the simulation scenario.

Second, there are ENodeB and UE models. ENodeB with MobilityHelper enbmobility is first created, and ENodeB location with Vector (enb\_X, enb\_Y, enb\_Z) is set. The numeric values of enb\_X, enb\_Y, and enb\_Z represent the location coordinate of the ENodeB in the X-axis, Y-axis, and Z-axis, respectively. Finally, the ENodeB mobility model, as ConstantPositionMobility-Model, is set to define that the ENodeB is constantly located in a fixed position. Concerning UE, the Mobility model is configured as ConstantVelocityMobility-Model to define that the UE is constantly moving at a fixed rate. The rate and direction of the motion of UE are set to SetVelocity(Vector(0, 300, 0)), signifying that UE is moving at 300m/s in the direction of the Y-axis.

Last, in Building Blockage models, during the simulation, building size varies according to the near-actual size in the map, as Google Earth is used to measure the size of the building. For the simulation, the building type is set as Building::Commercial, and all buildings are set to have no windows by setting the wall type as Building::ConcreteWithoutWindows. During the analysis, each of the buildings is assumed to be a two-story building by setting SetNFloors(2) for every building. To compensate for blockage components inside the building, such as humans, machinery, desks, and other clutterers, every building is assumed to have multiple rooms on both the X-axis and the Y-axis. These blockage components are set with SetNRoomsX(10) and SetNRoomsX(10), as the number of rooms on Xaxis and Y-axis vary depending on building size.

## J. Simulation Scenario

Concerning the simulation, the industrial complex is randomly selected with no specific criteria. The research uses Google Earth to find industrial complexes near Jakarta. The purpose of the simulation is to study the performance of Sub-TeraHertz signals in a real industrial environment. During the process, an industrial complex in Sentul is selected as the case study. The actual size and position of the building are mapped into NYUSIM as shadowing components.

In NS-3, each building is configured using Building Helper. The configuration is configured to mimic the actual object in real conditions. An example of an object building with a width of 100 m, a length of 140 m, and a height of 20 m is shown in Fig. 1. During the process, the building wall type is set to Building::Commercial and without windows. The building is a two-story building, and several rooms are available on each story. The number of rooms observed in the process represents the amount of scatterers.



Fig. 1. A real-world industrial complex taken from Google Earth.

An industrial complex in Fig. 1 represents a real-world high-density clutter area with multi-story buildings. Each building is also very close to another and comprises many shadowing components, such as rooms, machines, and other objects. Following the process, the researchers model the building position into a logical presentation to mimic its real-world actual position and size, as shown in Fig. 2.

Figure 3 illustrates a simulation scenario of UE mobility. In Scenario-1, UE moves outside the buildings. In this scenario, UE was assumed to move at constant velocity on the side of the road next to the buildings. The scenario was designed to simulate LOS and NLOS conditions and to review signal performance where the UE was outside of the buildings. In this context, UE experiences a decrease in signal quality due to blocking from surrounding buildings (NLOS) or may not experience any blocking at all due to the absence of buildings (LOS). Therefore, UE experienced various changes in signal quality due to the transition between NLOS and LOS, and vice versa.

In Scenario-2, UE moves on the second floor. In this situation, UE is assumed to move in constant motion on the second floor (11 m height) of the building. The scenario is designed to simulate the performance of Sub-TeraHertz inside and outside a building. In this context, UE experiences various signal quality changes due to switching from indoor to outdoor and vice versa (O2I loss). The signal quality received by the UE is affected by blockage from shadowing components, such as walls, roofs, and other blocking objects on the

second floor of the building.

In Scenario-3, UE moves on the first floor. In this scenario, UE is assumed to move in constant motion on the first floor (1 m height) of the building. The scenario is similar to Scenario-2 since they have similar transitions from indoor to outdoor and vice versa. However, the signal quality received by the UE experiences more shadow components compared to Scenario-2, because in this scenario, the UE suffers blockage from both scatterers on the first and second floors.

#### III. RESULTS AND DISCUSSION

In the research, several simulations are performed. They are divided into four parts. The first part is to simulate the center frequency at 73 GHz, and the second part is to activate the center frequency at 100 GHz. In addition, the third part is to simulate the center frequency at 120 GHz, and the fourth is to activate the center frequency at 140 GHz. Each part of the simulation consists of three scenarios, namely Scenario-1, 2, and 3. The purpose of this simulation is to study how mmWave as well as Sub-TeraHertz signals perform in high-density clutter areas and further analyze the comparative performance of Sub-TeraHertz signals for each of the bandwidth, frequency, and scenario. The results of each simulation scenario are analyzed using Signal-to-Noise Ratio (SNR) analysis, which is crucial since it considers both signal strength and noise level. This method is used to observe how signal performance is changed with varying parameters.

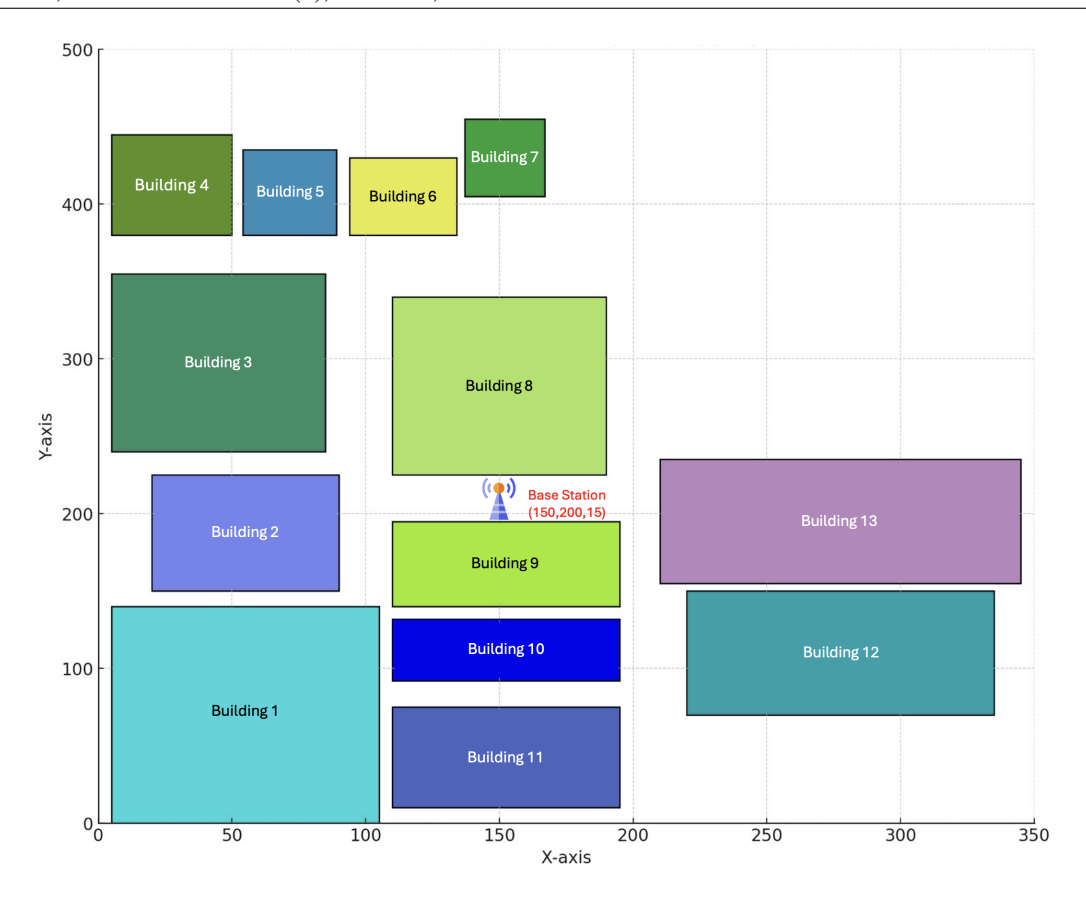


Fig. 2. The modeled representation of the industrial complex.

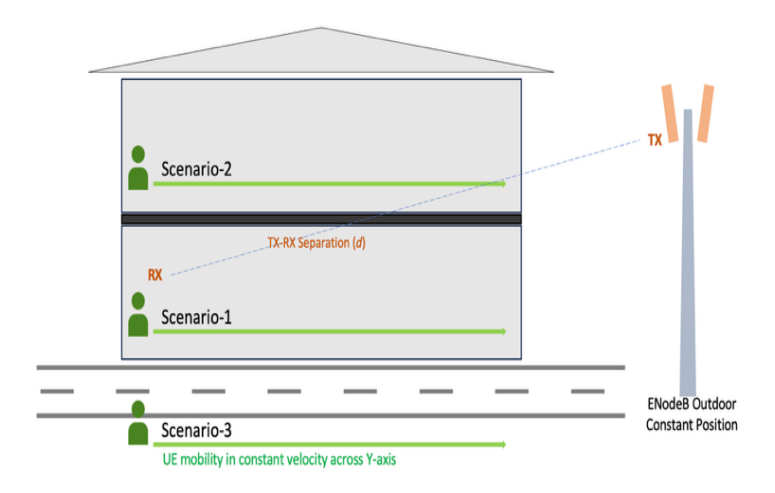


Fig. 3. User Equipment (UE) mobility scenario for simulations.

## A. Inter-Bandwidth Comparison

The simulation results are presented in Figs. 4–7. They illustrate the comparison of SNR performance across different bandwidth levels. The evaluation at a frequency of 73 GHz (Fig. 4) shows that the highest

SNR is achieved at the shortest distance between the UE and the eNodeB across all scenarios. As the distance increases, however, the SNR performance gradually declines, with the most pronounced degradation observed at the 800 MHz bandwidth. A similar trend

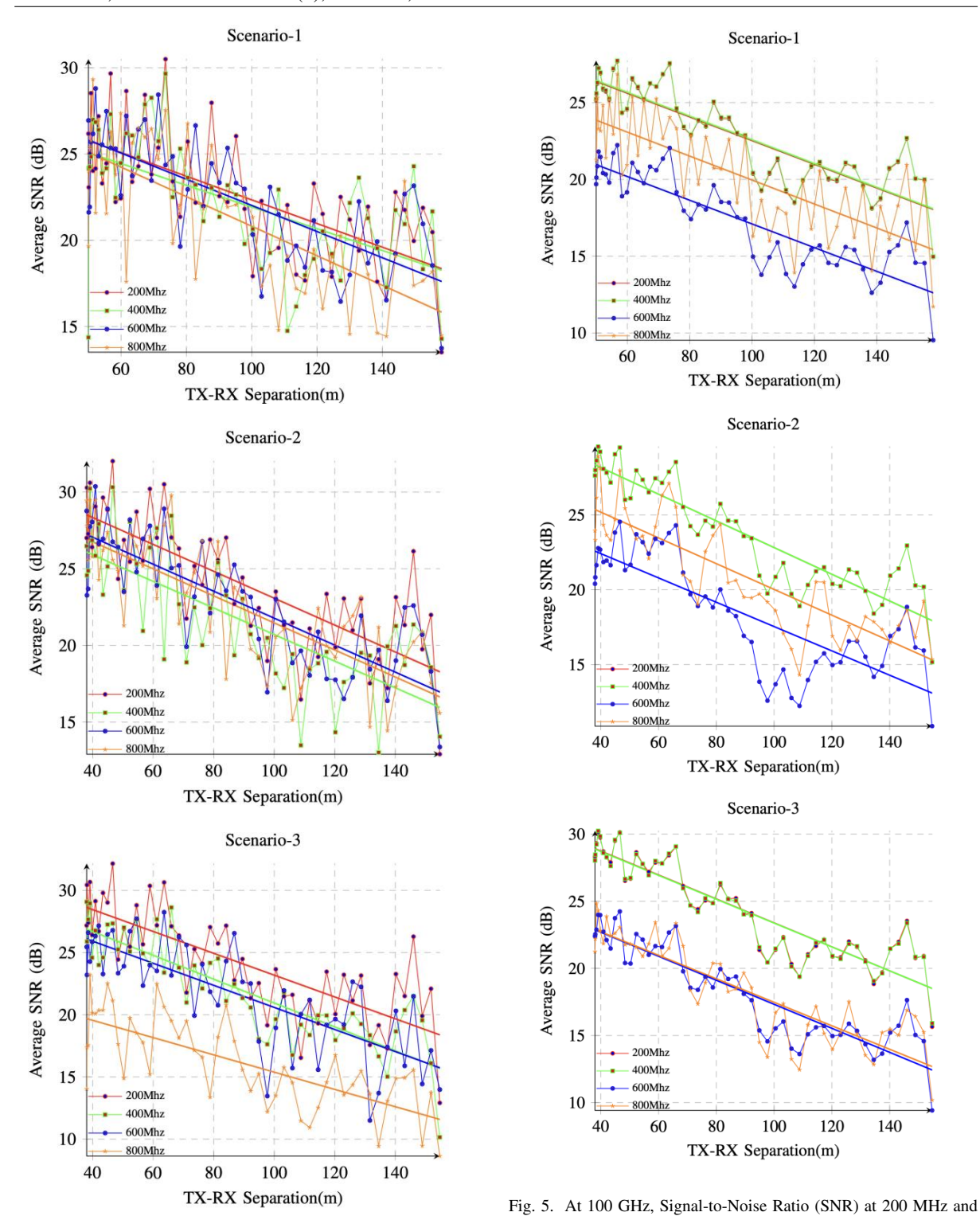


Fig. 4. Gradual decrease of Signal-to-Noise Ratio (SNR) with the wider spectrum bandwidth at 73 GHz. TX-RX means transmitter-receiver.

though the SNR performance at 200 MHz and 400 MHz bandwidths appears nearly identical.

400MHz being nearly identical. TX-RX means transmitter-receiver.

is evident in the 100 GHz evaluation (Fig. 5), al-

At 120 GHz (Fig. 6), the SNR values for the 200

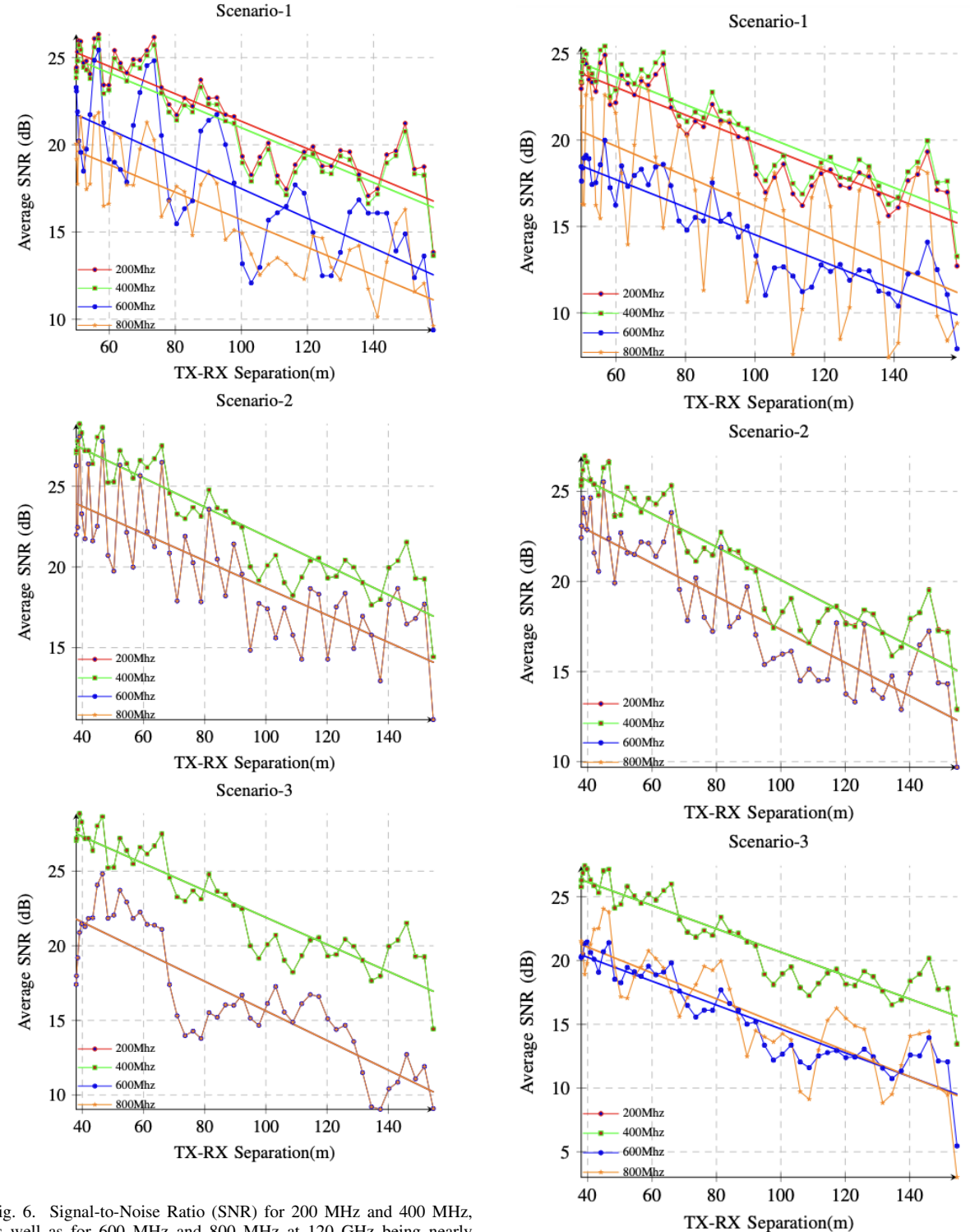


Fig. 6. Signal-to-Noise Ratio (SNR) for 200 MHz and 400 MHz, as well as for 600 MHz and 800 MHz at 120 GHz being nearly identical except for Scenario-1. TX-RX means transmitter-receiver.

Fig. 7. Inter-bandwidth Signal-to-Noise Ratio (SNR) pattern at 140 GHz being similar at 120 GHz. TX-RX means transmitter-receiver.

MHz and 400 MHz bandwidths differ only marginally, while the 600 MHz and 800 MHz bandwidths show a relatively more noticeable gap. This trend is also

observed in the evaluation at 140 GHz (Fig. 7). Overall, the slope of the SNR degradation across all tests

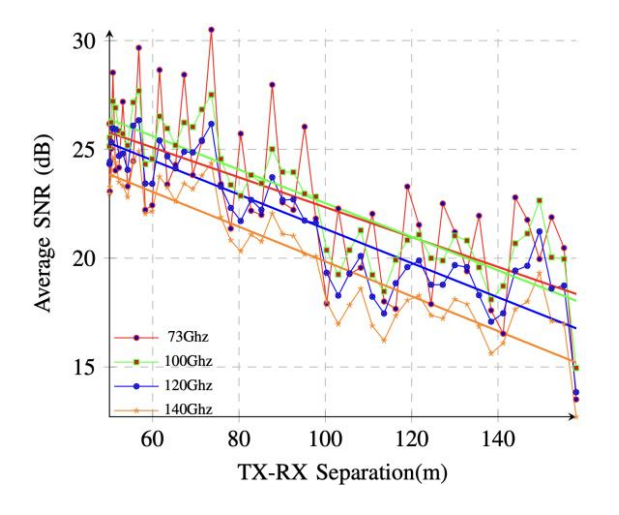


Fig. 8. Gradual decrease of Signal-to-Noise Ratio (SNR) as the higher frequency for all Scenario-1 at a constant 200 MHz bandwidth. TX-RX means transmitter-receiver.

indicates that the distance between the transmitter ENodeB and receiver UE exerts a significant influence on signal reception quality. The findings reveal that both increased distance between TX and RX and higher bandwidth levels contribute to reduced SNR performance.

The results signify that lower bandwidth produces better SNR than higher bandwidth. Although the differences between each bandwidth are not often uniform or linear, the bandwidths are important. For example, the inter-bandwidth SNR difference for Scenario-2 on 73G is relatively subtle. However, on other frequency bands, there is a significant difference. The simulation results also show that TX-RX distance greatly affects SNR. An additional distance of about 20 m leads to an SNR decrease of about 1 dB to 3 dB. It is also observed from the steep slope of the trend line of SNR. In Eq. (2), shown earlier, FSPL is a function of frequency and distance. The signal loss significantly increases when the frequency or distance improves. The noise level is also directly proportional to the bandwidth, while the signal power stays constant. This phenomenon explains the simulation results, as the analysis increases the bandwidth, the SNR gradually decreases.

#### B. Inter-Frequency Band Comparison

The comparative analysis is conducted to review how the frequency band affects the SNR performance. To review the comparison of signal reception performance, all simulation results of all simulated frequencies at the same bandwidth and scenario are combined. In the comparative analysis, the simulation results from all scenarios with a bandwidth of 200 MHz are shown

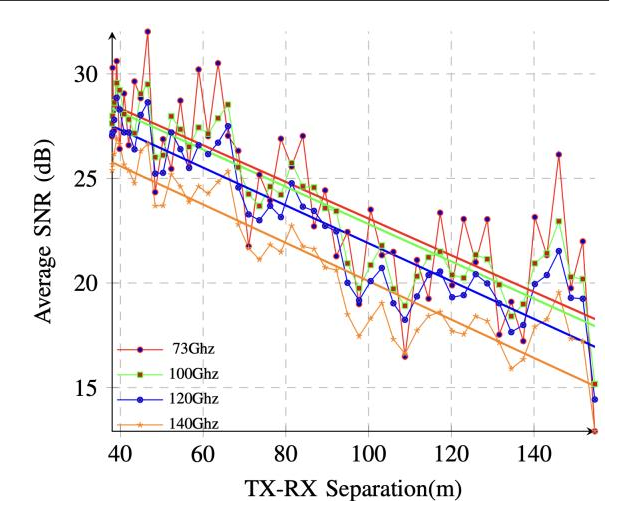


Fig. 9. Gradual decrease of Signal-to-Noise Ratio (SNR) as the higher frequency for all Scenario-2 at a constant 200 MHz bandwidth. TX-RX means transmitter-receiver.

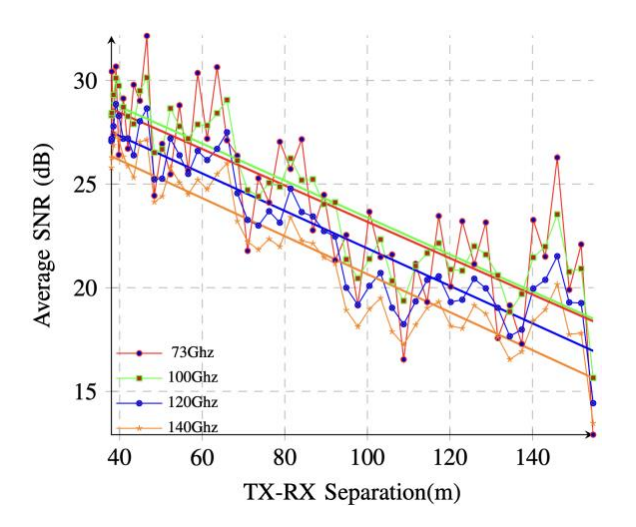


Fig. 10. Gradual decrease of Signal-to-Noise Ratio (SNR) as the higher frequency for all Scenario-3 at a constant 200 MHz bandwidth. TX-RX means transmitter-receiver.

in Figs. 8–10. Figure 8 presents the SNR performance at 200 MHz bandwidth under UE mobility Scenario-1. The results indicate that lower frequencies, particularly 73 GHz, achieve consistently higher SNR compared to higher carrier frequencies. The performance gap is most evident between 73 GHz, with SNR values exceeding 20 dB, and 140 GHz, where SNR falls below 15 dB. Although the rate of SNR degradation with distance is similar across frequencies, the overall trend confirms that increasing carrier frequency leads to reduced signal quality, with only minor differences observed between 73 GHz and 100 GHz.

Comparable trends are observed in Scenario-2

(Fig. 9) and Scenario-3 (Fig. 10). In both cases, SNR peaks above 25 dB at short distances (40 m) and declines steadily to around 15 dB at 140 m. This 10 dB reduction over a 100 m range underscores the strong influence of transmitter–receiver separation on mmWave signal reception. These findings highlight the critical role of eNodeB location planning in mitigating path loss and ensuring reliable coverage in mmWave networks. Furthermore, the fact that noticeable degradation is observed even at the narrowest tested bandwidth (200 MHz) demonstrates the inherent vulnerability of mmWave signals to distance-dependent attenuation.

It is concluded that lower frequencies provide higher average SNR than higher frequencies, although there is only a slight difference between 73 GHz and 100 GHz. Comparative analysis for other bandwidth classes also shows similar results and is consistent with these results. An explicit difference is observed at 120 and 140 GHz, although the SNR at 73 GHz, as well as at 100 GHz, tends to be similar across all scenarios. These results show that SNR performance remains stable at frequencies < 100 GHz. However, a significant decrease occurs after the frequency is less than 100 GHz. In all scenarios, a lower frequency produces a higher SNR than a higher frequency. The results show that SNR and the noise level highly depend on the frequency. Moreover, a substantial reduction in SNR is observed even when the bandwidth remains unchanging.

## C. Inter-Scenario Comparison

In the research, each UE mobility scenario is subjected to different blockage conditions, allowing for a comparative analysis of their impact on signal propagation. As shown in Fig. 3, the UE in Scenario-1 is anticipated to encounter more severe propagation blockage than in Scenario-2. It is primarily due to the greater number of rooms, walls, and floors that contribute additional path loss. By contrast, Scenario-3 is expected to exhibit lower blockage levels because the UE moves in an outdoor setting with fewer structural obstructions. Nonetheless, such expectations cannot be based solely on intuition. Systematic testing through simulation is essential to validate these assumptions and to accurately assess performance outcomes.

To ensure a valid comparison of signal reception across scenarios, the simulation results obtained at constant frequency bands and bandwidths are combined. The outcomes are presented in Figs. 11 and 12 for 73 GHz and 140 GHz, respectively. As shown in Fig. 11, the signal reception in Scenario-3 yields higher SNR values compared to both Scenario-1 and Scenario-2.

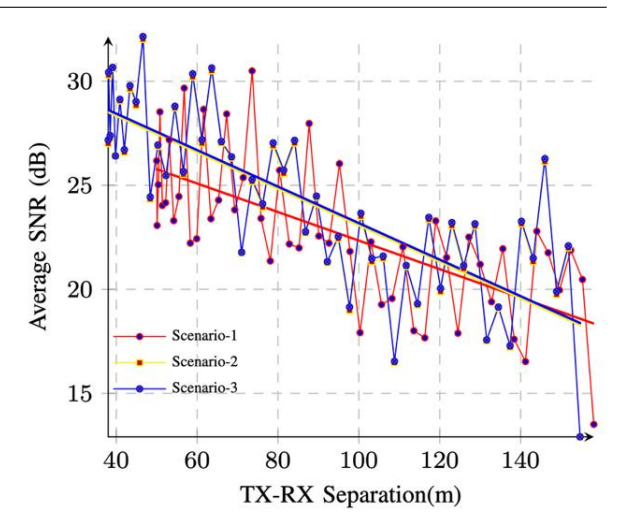


Fig. 11. Comparative Signal-to-Noise Ratio (SNR) performance inter User Equipment (UE) mobility scenarios at constant frequency 73 GHz and 200 MHz bandwidth. TX-RX means transmitter-receiver.

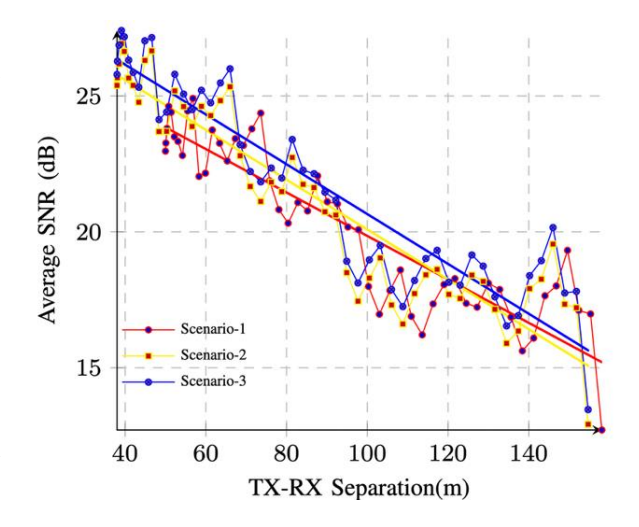


Fig. 12. Comparative Signal-to-Noise Ratio (SNR) performance inter User Equipment (UE) mobility scenarios at constant frequency 140 GHz and 200 MHz bandwidth. TX-RX means transmitter-receiver.

Although the SNR trend in Scenario-3 is only slightly higher than that of Scenario-2, the difference is sufficiently notable. Meanwhile, the gap with Scenario-1 is more substantial. Scenario-1 consistently demonstrates the weakest SNR performance, which aligns with prior expectations, given that this scenario is intentionally designed to experience greater blockage relative to the other two scenarios.

At the frequency of 140 GHz, as illustrated in Fig. 12, a similar trend is observed in which Scenario-3 consistently provides higher SNR performance compared to the other scenarios. However, a slight distinc-

tion can be noted, as the performance gap between Scenario-3 and Scenario-2 becomes more noticeable. This difference is nearly indistinguishable in the 73 GHz evaluation but becomes increasingly evident at 140 GHz. This finding suggests that as the carrier frequency increases, the performance disparities among scenarios become more clearly observable. Such behavior can be attributed to the frequency-dependent behavior of signal propagation, where higher frequencies experience greater path loss and are more susceptible to blockage and absorption by blockages. Consequently, minor structural differences between scenarios translate into more significant variations in SNR at higher frequencies, highlighting the critical importance of careful deployment planning when utilizing mmWave bands in dense environments such as industrial complex.

Across all evaluations, Scenario-3 consistently demonstrates the best SNR performance, followed by Scenario-2. Then, Scenario-1 yields the weakest results. These findings indicate that Scenario-1 is subject to a greater number of shadowing components at equivalent distances compared to the other scenarios. It is largely attributed to additional propagation losses introduced by multiple surrounding walls, rooms, and floor structures. In contrast, Scenario-3 exhibits significantly better performance, as the UE moves around the exterior of the building and avoids traversing its interior, where dense structural blockages are present. Scenario-2 provides intermediate results between the two extremes, as the UE signal reception is primarily influenced by blockages caused by walls and rooms located on the second floor of the building. Conversely, in Scenario-1, the received signal undergoes higher levels of path loss due to the combined effect of obstructions present on both the first and second floors.

From a theoretical perspective, these results can be explained by the principles of multipath propagation and penetration loss. In indoor environments, walls, floors, and other structural elements not only attenuate the signal but also generate reflected, scattered, and diffracted components. While some of these multipath components may constructively interfere and enhance signal reception, in dense indoor conditions, they often lead to destructive interference, further degrading the effective SNR. Moreover, as frequency increases, penetration loss through walls and floors becomes more severe, compounding the impact of blockages. Therefore, the observed differences between the scenarios are consistent with fundamental propagation theory, where structural density and frequency-dependent penetration losses are critical determinants of signal quality.

These findings provide a clear explanation for the common practice of deploying signal repeaters or indoor antennas within buildings. Such actions are planned to mitigate the disparity in signal reception quality that naturally emerges between outdoor and indoor settings. The simulations in the research reveal a significant gap in signal strength and quality between indoor and outdoor scenarios, highlighting the challenges of reliable indoor coverage. Furthermore, the results emphasize the importance of thorough planning in determining antenna placement within multistory buildings. The results underscore the necessity of hybrid deployment strategies, where both indoor and outdoor antenna systems are optimally positioned to ensure consistent coverage across all floors of a building.

Based on the three comparative analyses from the simulation results, it can be concluded that SNR performance is strongly influenced by bandwidth level, carrier frequency, and the number of blockages along the propagation path. The simulations demonstrate that these three variables collectively contribute to observable variations in SNR performance, even when observed at the exact transmission distance. Furthermore, the results reveal that relatively short distance variations (less than 100 m) can lead to significant differences in SNR reception. This finding highlights the prominent sensitivity of mmWave and sub-Terahertz to TX-RX separation, reinforcing the critical importance of precise distance and propagation environment considerations in the design and deployment of extremely high-frequency wireless networks.

#### IV. CONCLUSION

The research evaluates the performance of mmWave and Sub-TeraHertz signals in high-density clutter areas through simulation. NS-3 and NYUSIM modules are used as tools to simulate signals >100 GHz. Additionally, the simulation is designed to resemble real conditions that represent high-density areas, such as industrial complexes. The simulation results show that the frequency band, user movement (i.e., the number of shadowing components between the TX and RX), and spectrum bandwidth significantly affect the performance of the received signal at the RX side, in addition to the TX-RX distance.

Despite mmWave and Sub-TeraHertz communications offering influential advantages, the models also raise comparable concerns. The research shows that signal quality highly depends on frequency, bandwidth, distance, atmospheric losses, and the existence of blockages. The research shows that mmWave and Sub-TeraHertz communications face significant challenges in high-density industrial environments due to the density of various objects. However, the need for

capacity-hungry communication in dense areas such as industrial areas is rising, and mmWave as well as Sub-TeraHertz can be an ideal choice.

Future studies on mmWave and Sub-Terahertz wireless communication should focus on overcoming the inherent challenges of outdoor-to-indoor reception, severe blockage, and wireless network design in dense environments. At these extremely high frequencies, signals experience substantial penetration loss through walls, floors, and windows, resulting in significantly weaker indoor coverage compared to outdoor reception. To address this issue, future studies can explore advanced penetration models and design distributed antenna systems to mitigate blockage and extend coverage indoors. Furthermore, research should emphasize hybrid network architectures that integrate outdoor cells with indoor repeaters. Such strategies are essential for guaranteeing robust and seamless connectivity in dense environments and multi-story building scenarios, where the limitations of mmWave and sub-THz systems are most observable.

#### **AUTHOR CONTRIBUTION**

Proposed main idea of the project and drafted initial guidance for the simulations, I. D. P. M.; Supervised tools preparation and performed simulation and data collection, I. D. P. M.; Contributed data visualization, I. D. P. M.; Provided data interpretation and analysis, I. D. P. M.; Drafted initial reports and supervised the report completion, I. D. P. M.; Prepared tools, ran and tested the simulation, and collected the data, R. H. H. S.; Provided location maps and modeled it into logical representation, R. H. H. S.; Conducted simulation result analysis, impacts, and interpretation, R. H. H. S.; Drafted initial paper and contributed to the literature review, R. H. H. S.; Recorded all the data results from the simulation, I. R. D. B.; Proposed custom simulation to broaden the analysis, I. R. D. B.; Finalized report, I. R. D. B.; Proposed guidance on the analysis and interpretation of the results, R. F. S.; and Supervised the project and reviewed the data collection, analysis, and research writing, R. F. S.

#### DATA AVAILABILITY

The data that support the findings of the research are openly available in GitHub at https://github.com/IwanManurung/Performance-Evaluation-of-mmWave-and-Sub-TeraHertz-Using-NYUSIM

#### REFERENCES

[1] Y. Niu, Y. Li, D. Jin, L. Su, and A. V. Vasilakos, "A survey of millimeter wave communications (mmWave) for 5G: Opportunities and

- challenges," *Wireless networks*, vol. 21, no. 8, pp. 2657–2676, 2015.
- [2] H. Poddar, T. Yoshimura, M. Pagin, T. S. Rappaport, A. Ishii, and M. Zorzi, "Full-stack endto-end mmWave simulations using 3GPP and NYUSIM channel model in NS-3," in *ICC 2023-IEEE International Conference on Communications*. Rome, Italy: IEEE, May 28–June 1, 2023, pp. 1048–1053.
- [3] V. Petrov, T. Kurner, and I. Hosako, "IEEE 802.15. 3d: First standardization efforts for subterahertz band communications toward 6G," *IEEE Communications Magazine*, vol. 58, no. 11, pp. 28–33, 2020.
- [4] H. Mi, B. Ai, R. He, T. Wu, X. Zhou, Z. Zhong, H. Zhang, and R. Chen, "Multi-scenario millimeter wave channel measurements and characteristic analysis in smart warehouse at 28 GHz," *Electronics*, vol. 12, no. 15, pp. 1–14, 2023.
- [5] A. A. A. Boulogeorgos, A. Alexiou, T. Merkle, C. Schubert, R. Elschner, A. Katsiotis *et al.*, "Terahertz technologies to deliver optical network quality of experience in wireless systems beyond 5G," *IEEE Communications Magazine*, vol. 56, no. 6, pp. 144–151, 2018.
- [6] S. Ju and T. S. Rappaport, "142 GHz multipath propagation measurements and path loss channel modeling in factory buildings," in *ICC 2023-IEEE International Conference on Communica*tions. Rome, Italy: IEEE, May 28–June 1, 2023, pp. 5048–5053.
- [7] F. Zhang, M. F. Bengtson, P. Kyösti, J. Kyröläinen, and W. Fan, "Dynamic sub-THZ radio channel emulation: Principle, challenges, and experimental validation," *IEEE Wireless Communications*, vol. 31, no. 1, pp. 10–16, 2024.
- [8] B. K. J. Al-Shammari, I. Hburi, H. R. Idan, and H. F. Khazaal, "An overview of mmWave communications for 5G," in 2021 International Conference on Communication & Information Technology (ICICT). Basrah, Iraq: IEEE, June 5–6, 2021, pp. 133–139.
- [9] M. Polese, X. Cantos-Roman, A. Singh, M. J. Marcus, T. J. Maccarone, T. Melodia, and J. M. Jornet, "Coexistence and spectrum sharing above 100 GHz," *Proceedings of the IEEE*, vol. 111, no. 8, pp. 928–954, 2023.
- [10] M. Jacob, S. Priebe, R. Dickhoff, T. Kleine-Ostmann, T. Schrader, and T. Kurner, "Diffraction in mm and sub-mm wave indoor propagation channels," *IEEE Transactions on Microwave Theory and Techniques*, vol. 60, no. 3, pp. 833–844,

2012.

- [11] O. Kanhere, H. Poddar, Y. Xing, D. Shakya, S. Ju, and T. S. Rappaport, "A power efficiency metric for comparing energy consumption in future wireless networks in the millimeter-wave and terahertz bands," *IEEE Wireless Communications*, vol. 29, no. 6, pp. 56–63, 2022.
- [12] H. Abdellatif, V. Ariyarathna, A. Madanayake, and J. M. Jornet, "A real-time software-defined radio platform for sub-terahertz communication systems," *IEEE Access*, vol. 12, pp. 146315–146327, 2024.
- [13] P. Li, J. Wang, L. Zhao, X. Gao, F. Song, H. Sun, and J. Ma, "Scattering and eavesdropping in terahertz wireless link by wavy surfaces," *IEEE Transactions on Antennas and Propagation*, vol. 71, no. 4, pp. 3590–3597, 2023.
- [14] M. K. Samimi and T. S. Rappaport, "3-D millimeter-wave statistical channel model for 5G wireless system design," *IEEE Transactions on Microwave Theory and Techniques*, vol. 64, no. 7, pp. 2207–2225, 2016.
- [15] M. Mezzavilla, S. Dutta, M. Zhang, M. R. Akdeniz, and S. Rangan, "5G mmWave module for the NS-3 network simulator," in *Proceedings of the 18<sup>th</sup> ACM International Conference on Modeling, Analysis and Simulation of Wireless and Mobile Systems*, Cancun, Mexico, Nov. 2 6, 2015, pp. 283–290.
- [16] nsnam, "Documentation." [Online]. Available: https://www.nsnam.org/documentation/
- [17] N. Baldo, "The NS-3 LTE module by the LENA project." [Online]. Available: https://www.nsnam.org/tutorials/consortium13/lte-tutorial.pdf
- [18] NS-3 App Store, "ndnSIM: Named-Data Networking (NDN) Simulator." [Online]. Available: https://apps.nsnam.org/app/ndnsim/
- [19] S. Sun, G. R. MacCartney, and T. S. Rappaport, "A novel millimeter-wave channel simulator and applications for 5G wireless communications," in 2017 IEEE international conference on communications (ICC). Paris, France: IEEE, May 21–25, 2017, pp. 1–7.
- [20] E. Dervisevic, M. Voznak, and M. Mehic, "Large-scale quantum key distribution network simulator," *Journal of Optical Communications and Networking*, vol. 16, no. 4, pp. 449–462, 2024.
- [21] nsnam, "Related project." [Online]. Available: https://www.nsnam.org/wiki/Related\_Projects
- [22] H. Poddar, T. Yoshimura, M. Pagin, T. Rappaport, A. Ishii, and M. Zorzi, "NS-3 implementation of sub-terahertz and millimeter wave drop-based NYU channel model (NYUSIM)," in *Proceedings*

- of the 2023 Workshop on NS-3. Arlington VA, USA: Association for Computing Machinery, June 28–29, 2023, pp. 19–27.
- [23] H. Poddar, "NYUSIM wireless channel simulator extension above 100 GHz and implementation in NS-3," Master's thesis, New York University Tandon School of Engineering, 2023.
- "5G; Study [24] ETSI, on channel model for frequencies from 0.5 to 100 GHz (3GPP TR 38.901 version 14.3.0 Release 14)," 2018. [Online]. Available: https: //www.etsi.org/deliver/etsi tr/138900 138999/ 138901/14.03.00\_60/tr\_138901v140300p.pdf
- [25] T. S. Rappaport, Y. Xing, O. Kanhere, S. Ju, A. Madanayake, S. Mandal, A. Alkhateeb, and G. C. Trichopoulos, "Wireless communications and applications above 100 GHz: Opportunities and challenges for 6G and beyond," *IEEE Access*, vol. 7, pp. 78729–78757, 2019.
- [26] M. K. Samimi, T. S. Rappaport, and G. R. Mac-Cartney, "Probabilistic omnidirectional path loss models for millimeter-wave outdoor communications," *IEEE Wireless Communications Letters*, vol. 4, no. 4, pp. 357–360, 2015.
- [27] H. Poddar, S. Ju, D. Shakya, and T. S. Rappaport, "A tutorial on NYUSIM: Sub-terahertz and millimeter-wave channel simulator for 5G, 6G, and beyond," *IEEE Communications Surveys & Tutorials*, vol. 26, no. 2, pp. 824–857, 2023.
- [28] M. González-Palacio, D. Tobón-Vallejo, L. M. Sepúlveda-Cano, S. Rúa, and L. B. Le, "Machine-learning-based combined path loss and shadowing model in LoRaWAN for energy efficiency enhancement," *IEEE Internet of Things Journal*, vol. 10, no. 12, pp. 10725–10739, 2023.
- [29] S. Sun, T. S. Rappaport, M. Shafi, P. Tang, J. Zhang, and P. J. Smith, "Propagation models and performance evaluation for 5G millimeterwave bands," *IEEE Transactions on Vehicular Technology*, vol. 67, no. 9, pp. 8422–8439, 2018.
- [30] Y. Yoon and H. J. Park, "Excess loss by urban building shadowing and empirical slant path model," *IEEE Antennas and Wireless Propagation Letters*, vol. 21, no. 2, pp. 237–241, 2021.
- [31] M. Olyaee, H. Hashemi, and J. M. Romero-Jerez, "Performance analysis under the Independent Fluctuating Two-Ray (IFTR) fading in RIS-assisted millimeter wave communications," in 2024 32<sup>nd</sup> International Conference on Electrical Engineering (ICEE). Tehran, Islamic Republic of Iran: IEEE, May 14–16, 2024, pp. 1–5.
- [32] O. J. G. Al-Qadi, B. A. Tazifua, and E. S. Semenov, "Analysis of discrete message transmis-

- sion in orthogonal frequency division multiplexing systems," *NBI technologies*, vol. 16, no. 4, pp. 5–9, 2022.
- [33] A. E. C. Redondi, C. Innamorati, S. Gallucci, S. Fiocchi, and F. Matera, "A survey on future millimeter-wave communication applications," *IEEE Access*, vol. 12, pp. 133 165–133 182, 2024.
- [34] I. Picallo, P. L. Iturri, M. Celaya-Echarri, L. Azpilicueta, and F. Falcone, "Deterministic wireless channel characterization towards the integration of communication capabilities to enable context aware industrial Internet of Thing environments," *Mobile Networks and Applications*, vol. 28, no. 1, pp. 4–18, 2023.
- [35] G. R. MacCartney, T. S. Rappaport, and S. Rangan, "Rapid fading due to human blockage in pedestrian crowds at 5G millimeter-wave frequencies," in *GLOBECOM 2017-2017 IEEE Global Communications Conference*. Singapore: IEEE, Dec. 4–8, 2017, pp. 1–7.